Electronic Structure and Stability of Fluorophore–Nitroxide Radicals from Ultrahigh Vacuum to Air Exposure

ARTICLE *in* ACS APPLIED MATERIALS & INTERFACES · DECEMBER 2014

Impact Factor: 6.72 · DOI: 10.1021/am508854u · Source: PubMed

6 AUTHORS, INCLUDING:

Reza Kakavandi
Philipps University of Marburg
4 PUBLICATIONS **17** CITATIONS
SEE PROFILE

Prince Ravat
Max Planck Institute for Polymer Research
13 PUBLICATIONS **37** CITATIONS
SEE PROFILE

Yulia B. Borozdina
University of Greifswald
8 PUBLICATIONS **17** CITATIONS
SEE PROFILE

Martin Baumgarten
Max Planck Institute for Polymer Research
281 PUBLICATIONS **4,365** CITATIONS
SEE PROFILE

ACS APPLIED MATERIALS & INTERFACES

Research Article

www.acsami.org

Electronic Structure and Stability of Fluorophore–Nitroxide Radicals from Ultrahigh Vacuum to Air Exposure

R. Kakavandi,[†] P. Ravat,[‡] S.-A. Savu,[†] Y. B. Borozdina,[‡,§] M. Baumgarten,[‡] and M. B. Casu*[,†]

[†]Institute of Physical and Theoretical Chemistry, University of Tübingen, Auf der Morgenstelle 18, D-72076 Tübingen, Germany

[‡]Max Planck Institute for Polymer Research, Ackermannweg 10, D-55128 Mainz, Germany

Supporting Information

ABSTRACT: Thin film processes of organic radicals remain widely unknown, although these materials may have a significant technological potential. In aiming at their use in applications, we explore the electronic structure of thin films of a nitronyl nitroxide radical attached to a fluorophore core. According to our findings, this molecule maintains its radical function and, consequently, its sensing capabilities in the thin films. The films are characterized by a high structural degree of the molecular arrangement, coupled to strong vacuum and air stability that make this fluorophore–nitroxide radical an extremely promising candidate for application in electronics. Our work also identifies a quantitative correlation between the results obtained by the simultaneous use of X-ray photoemission and electron paramagnetic resonance spectroscopy. This result can be used as a standard diagnostic tool in order to link the (in situ-measured) electronic structure with classical ex situ paramagnetic investigations.

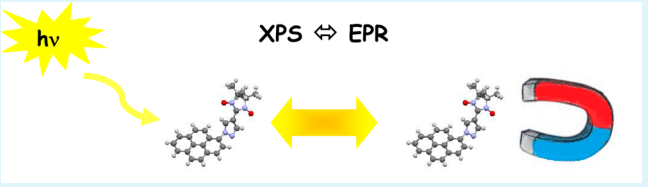

KEYWORDS: *nitronyl nitroxides, X-ray photoelectron spectroscopy, electron paramagnetic resonance spectroscopy, magnetism, thin film growth, organic paramagnets on surfaces*

INTRODUCTION

The success of organic electronics is an indisputable reality that brought new devices on the market in a very short period of time since the successful demonstration of the first device performed by Tang and VanSlyke.[1] The huge progress in the field of organic electronics depends not only on the development of new devices and design optimization but also on the strength of synthetic chemistry. The structural variability of organic compounds allows for materials with specific characteristics that match the device requirements. However, single molecule characteristics may substantially differ in a nontrivial way when molecules are packed in solid thin films, or if they interact with a substrate.[2] Consequently, organic thin films and organic/inorganic interfaces remained in the focus of extensive investigations for two decades.[3−12] Very recently, the interest in this type of interfaces has enjoyed a renaissance with the flourishing of a body of work aiming at the deep comprehension of the interface mechanisms.[13−16] The variety of investigated organic systems is astonishingly large and includes pentacene, perylene and their derivatives,[3,4,17−19] the family of phthalocyanines,[20,21] and a great number of polymers.[22] Surprisingly, in comparison, little attention has been drawn to the study of thin films and interface properties of organic radicals.[23−31] The reason is that radicals are usually considered unstable. Indeed, this is true but not necessarily general: nitronyl and imino nitroxides are a class of stable materials discovered in 1968.[32] The most fascinating characteristic of nitronyl nitroxide radicals is that they are paramagnetic compounds bearing unpaired electrons localized mainly in the two NO groups.[25,33−35] Recently, they have been studied because of their use as a building block in more complex magnetic structures[36,37] and their redox characteristic that has been proposed to be exploitable in memory elements.[38] However, their thin film processes remain widely unknown, although these materials may have an immense technological potential.[34] In our previous work, we demonstrated by using X-ray photoelectron spectroscopy (XPS) and electron paramagnetic resonance (EPR) spectroscopy that we are able to evaporate without degradation[39] a pyrene derivative of the nitronyl nitroxide radical (4,4,5,5-tetramethyl-2-(pyrenyl)-imidazoline-1-oxy-3-oxide, NitPyn, see Scheme 1) and to grow its thin films on silicon,[40] silicon dioxide,[41] sapphire,[42] and titanium dioxide,[43,44] i.e., technologically relevant surfaces.

In the present work, we use soft X-ray techniques such as XPS and near edge X-ray absorption fine structure (NEXAFS) spectroscopy in combination with EPR measurements to explore in situ the electronic structure of thin films of 1-[4′-(3-oxide-1-oxyl-4,4,5,5-tetramethylimidazolin-2-yl)pyrazol-1′-yl]pyrene[45] (PPN, Scheme 1) deposited on SiO_2/Si(111), and ex situ the persistence of the paramagnetic character of the molecules in the thin films. A nitroxide free radical coupled to a fluorophore suppresses the normal fluorescence emission process.[46] In such a molecule, the nitroxides are efficient quenchers of the fluorescence, due to the relaxation of the fluorophore excited states caused by electron-exchange interactions with the radical.[47−49] On the one hand, PPN is a

Received: October 20, 2014
Accepted: December 18, 2014
Published: December 18, 2014

DOI: 10.1021/am508854u
ACS Appl. Mater. Interfaces 2015, 7, 1685−1692

Scheme 1. PPN Molecular Structure[a]

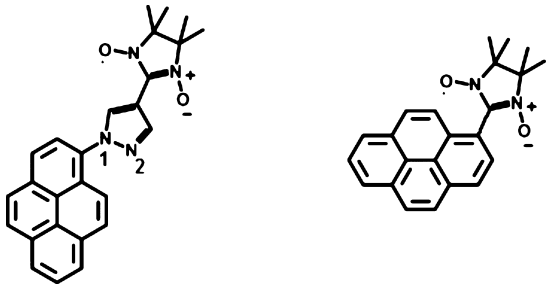

[a]The NitPyn molecular structure is also shown for comparison.

pyrene derivative of the nitronyl nitroxide radical that shows interesting properties as a redox probe, due to the attachment of a pyrazole ring that significantly enhances the n–π^* transition components of the absorption envelope of the radical. On the other hand, according to thermodynamics,[10,50,51] we expect that the presence of the pyrazole ring contributes to decreasing the molecule vapor pressure, leading to good film forming properties.[39] Since PPN sensing capabilities have been previously demonstrated,[45] exploring its thin film properties is of technological interest.

EXPERIMENTAL SECTION

PPN was synthesized according to the procedure reported in ref 45. Thin films of PPN were deposited in situ under UHV conditions by OMBD using a Knudsen cell (evaporation rate = 0.6 Å/min, substrate at room temperature (RT)). The evaporation rate was determined by a quartz microbalance and the nominal thickness was cross-checked by using the attenuation of the XPS substrate signal (Si 2p) after PPN deposition. Native SiO_2, grown on single-side polished p-Si(111) wafers with a doped resistivity of 5–10 Ω·cm (boron-doped) was employed as a substrate. Without any previous ex situ treatment, the clean substrates were prepared by outgassing in UHV by multiple cycles of annealing at around 500 K (i.e., much below the temperature at which the oxide is removed) for several hours with cleanness monitored by XPS and NEXAFS. The XPS experiment was performed in a UHV system equipped with a Specs Phoibos 150 analyzer and a monochromatic Al Kα source and at the UE52-PGM undulator beamline at the third generation synchrotron radiation facility BESSY II (Berlin). The UE52-PGM end-station had separated preparation and analysis chambers (base pressure = 2×10^{-10} mbar), equipped with a SCIENTA R4000 electron energy analyzer for high quality photoemission experiments. The synchrotron measurements were carried out in low-alpha (ring current at injection = 13/60 mA (mode B/mode A), cff = 2.5, analyzer resolution = 0.1 eV). The peak fit analysis was carried out with the Unifit package.[52] The NEXAFS spectra were measured in total and partial electron yield, normalized by the clean substrate signals. All spectra were scaled in order to give an equal edge jump.[10]

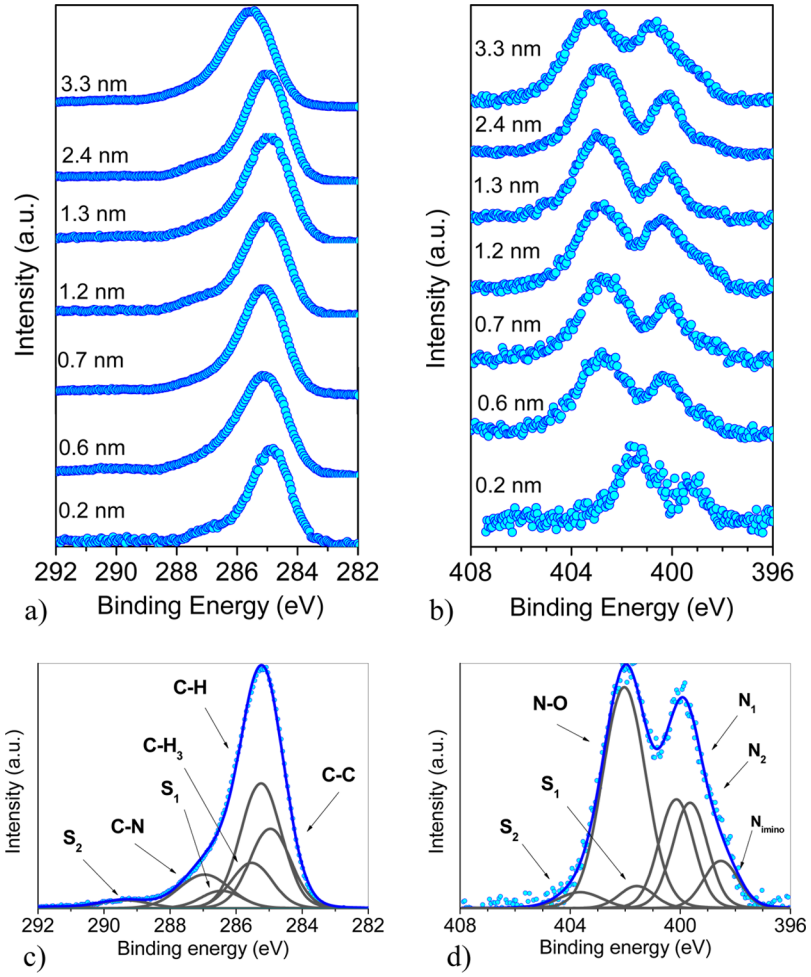

Figure 1. Thickness dependent C 1s (a) and N 1s (b) core level spectra of PPN thin films deposited on SiO_2/Si(111) surfaces. The peak-fit analysis for the 3.3 nm nominally thin film is also shown (c and d).

DOI: 10.1021/am508854u
ACS Appl. Mater. Interfaces 2015, 7, 1685–1692

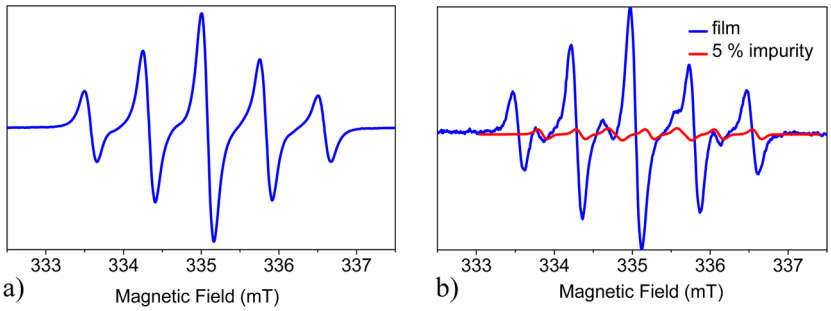

Figure 2. (a) EPR spectrum obtained from the solution of the PPN residual powders present in the cell after several cycles of evaporation. (b) EPR spectrum of a solution obtained from washing one of the thin films with toluene.

The EPR spectra were recorded in powders and diluted and oxygen-free solution of toluene (because of the different setup between the XPS and the EPR measurements) by using a Bruker X-band spectrometer ESP300 E, equipped with an NMR gauss meter (Bruker ER035), a frequency counter (Bruker ER041XK) and a variable temperature control continuous flow N_2 cryostat (Bruker B-VT 2000). The *g*-factor corrections were obtained by using DPPH ($g = 2.0037$) as the standard. The spectral simulations were carried out using WINEPR SimFonia software.

RESULTS AND DISCUSSION

The first aspect that we intend to address by XPS is whether it is possible to use organic molecular beam deposition (OMBD) to evaporate PPN under controlled conditions without molecular degradation. For this purpose, we measure the core level spectra of PPN thin films deposited on SiO_2/Si(111) surfaces shown in Figure 1, and analyze the elemental composition. This is possible due to the fact that the XPS signal intensity, given the photon energy, is proportional to the photon flux, the photoionization cross section, the number of photoemitting atoms, the transmission of the spectrometer, and the detection efficiency.[53] Consequently, the integrated signal intensities obtained analyzing the XPS curves are proportional to the molecular elemental composition. In the present case, we concentrate on the C/N ratio because of the presence of oxygen atoms in the substrate. From the XPS curves, we calculate a C/N ratio (6.2) that correlates very closely with the expected stoichiometric ratio (6.5). This means that the stoichiometry of the deposited films corresponds to the quantitative composition of the molecule, indicating a successful deposition. This result is confirmed by acquiring the same spectra on PPN powder embedded in indium foil (see the Supporting Information).

To further support this finding, we perform EPR measurements on the residual powder left in the Knudsen cell after undergoing several cycles of heating/evaporation. The EPR spectrum exhibits an isotropic five line pattern due to the presence of the two equivalent nitrogen nuclei of the imidazolyl moiety (Figure 2a).[54,55] The relative intensity of the lines follows the typical 1:2:3:2:1 pattern. This result indicates that the evaporation does not affect the nitronyl nitroxide radical.

Looking in detail at the core level spectra of a PPN film by using a best fit procedure, we can gain further information (Figure 1). The C 1s spectroscopic line is due to chemically inequivalent carbon sites that should yield, in principle, a different contribution to the spectrum. However, the small differences in binding energy, the limits imposed by the line width, and by the resolution of our experiment would make their identification by fitting quite speculative. Thus, the analysis is restricted to the contributions of aromatic carbon atoms (differentiating among C−C or C−H carbon atoms), methyl carbon atoms, and carbon atoms bound to nitrogen atoms, following the procedure discussed in ref 39, applying constraints based on stoichiometry and electronegativity. The fit results obtained from the analysis of the C 1s spectra show that the single contributions respect the stoichiometry of the molecule (see Figure 1 and tables in the Supporting Information). However, the most important information from the point of view of the radical intactness is related to the N 1s core level spectra. At least two main features should appear in the spectra as a consequence of the different chemical environment experienced from the nitrogen atoms belonging to the nitronyl nitroxide radical and the nitrogen atoms belonging to the pyrazole ring. In fact, the N 1s spectra are characterized by two main lines at 399.9 and 401.9 eV. The fitting procedure identifies not only the NO-related contribution, but we are also able to identify the two lines that differ in binding energy due to the electrons emitted from N1 and N2 nitrogen atoms of the pyrazole ring, in agreement with previously published works.[56−59] We observe additional contributions that we assign to the expected shakeup satellites, as response of the system to the core−hole creation, and a further contribution at around 398.7 eV corresponding to around 5/6% of the total intensity in the binding energy range. Its lower binding energy indicates that the chemical environment of the contributing nitrogen atoms is less electronegative than it is expected for nitrogen atoms of the intact nitronyl nitroxide radical and of the pyrazole nitrogen atoms. This observation indicates that a part of the molecules, namely around 6%, may undergo radical degradation either because of deposition or radiation exposure. Note that we take all possible precautions while measuring the films, and we are able to clearly identify slow degradation processes (on the time scale of around 4 min) related to beam exposure, if they occur.[39,41] However, we cannot completely exclude fast radiation damage. To shed light on the nature of this contribution, we perform EPR measurements on the solution obtained by washing the organic layers from the substrate with toluene. These provide spectra characterized by the same pattern as discussed above, and some additional features (Figure 2), related to the presence of the imino nitroxide radical. A spectral simulation[60] of the mixture of nitronyl nitroxide (5 lines with two equivalent nitrogens) and imino nitroxide (7 line feature from two different nitrogen hyperfine couplings) and their added sum leads to an estimate of approximately 5% impurity of imino nitroxide (Figure 2b). The agreement with the XPS results is astonishing, and this allows us assigning the contribution at 398.7 eV to the presence of a small amount of PPN molecules that underwent the release of an oxygen atom, converting to

DOI: 10.1021/am508854u
ACS Appl. Mater. Interfaces 2015, 7, 1685−1692

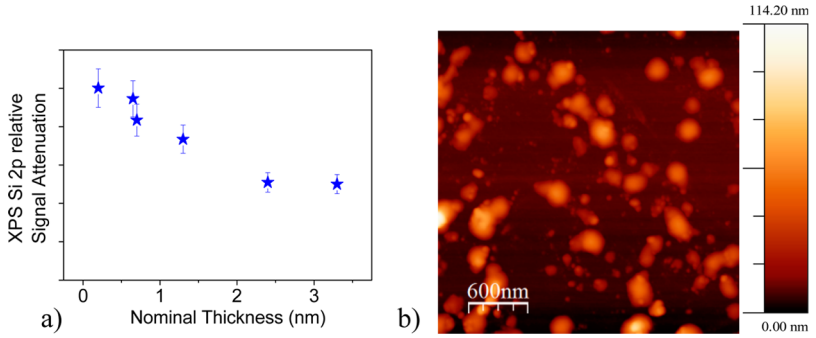

Figure 3. (a) Attenuation of the Si 2p XPS signal, normalized to the corresponding saturation signal, as a function of time during PPN deposition at RT. (b) Typical 3 × 3 μm AFM image of a 12 nm nominally thin film.

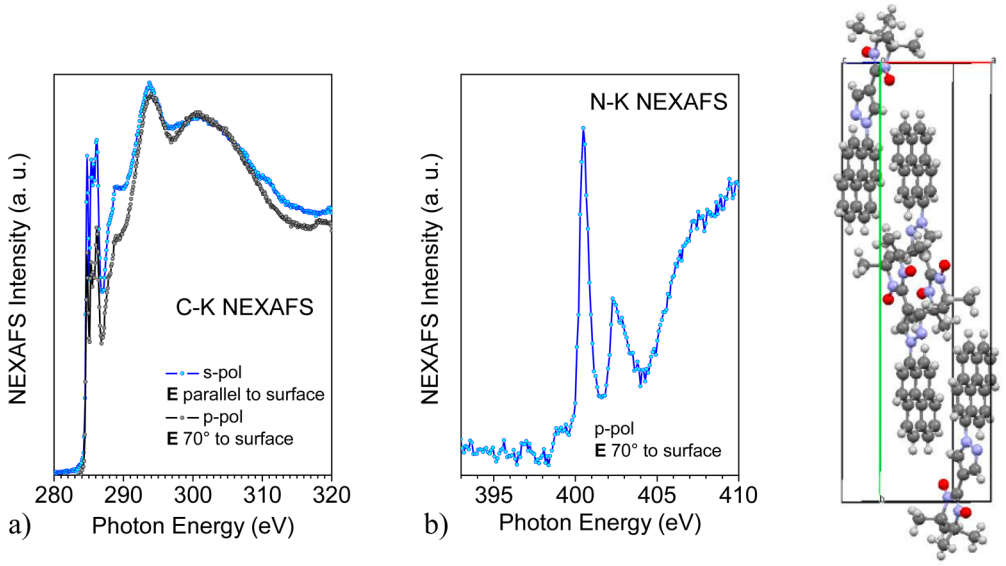

Figure 4. (a) C−K and (b) N−K edge NEXAFS spectra obtained from a 12 nm nominally thin film. The spectra were taken in grazing incident for two different polarization directions of the incident light, s-pol and p-pol, as indicated. The unit cell of PPN is also shown: the *b*-axis is the long axis.

the imino nitroxide radical. Therefore, we can conclude that evaporation and deposition of PPN under controlled conditions is possible without degradation (within the presence of around 5% impurities in the solid state).

The second aspect that we intend to address with XPS is the interaction between the PPN molecules and the substrate. Comparing the thin film spectra with the thick film spectra (Figure 1), we note that, apart from a shift of the spectroscopic lines toward higher binding energies, the shape of the spectra does not change with thickness. This observation hints at the physisorption of the molecules on SiO_2, because chemisorptions would significantly modify the photoemission features of the molecular assemblies close to the interface.[13,14] The shift is due to the fact that the screening of the core hole in the layer on top of the substrate is assisted by the substrate. Efficient screening is expected at the metal/organic interface owing to the occurrence of an image potential and, recently, it has been revealed also at the metal oxide/organic interface,[61,62] in agreement with our observation. Note that a slight different inhomogeneous broadening is visible with increasing thickness, especially in the N 1s core level spectra. This may be due to a different morphological and structural environment in the films at different thicknesses.[9]

The final aspect that we intend to address by using photoemission is the growth mode of PPN thin films under the present preparation conditions. This can be done analyzing the XPS signal substrate decay upon PPN deposition (Figure 3a). The attenuation curve shows two different slopes with a crossover between two regimes that corresponds to a nominal thickness of 0.7 nm. The intensity decay indicates Stranski-Krastanov growth mode and it is consistent with the atomic force microscopy (AFM) results (Figure 3b) clearly showing films with island morphology.

To investigate the PPN film structure and gain information on the unoccupied states, we use NEXAFS spectroscopy. The polarization dependent C−K edge spectra give information mostly on the pyrene orientation with respect to the substrate. We note that the C−K edge NEXAFS spectra of PPN thick films for two different polarization directions of the incident light, as indicated, (Figure 4) are characterized by the presence of a rich resonance structure. By analogy to the NEXAFS spectra of pyrene and pyrene-based molecules,[63,64] we identify two main regions: the π^* region up to 290 eV and the σ^* region in the photon energy range above 290 eV. In particular, four resonances are visible at 284.8, 285.4, 285.7, and 286.2 eV; they are due to transitions from C 1s levels mainly into the lowest unoccupied molecular orbitals (LUMOs). They have a C═C character. The peaks at 287.8 and 288.9 eV have presumably a mixed character (σ^*(C−H) and π^*(C═C)). Finally, the features above 290 eV have also a mixed nature due

DOI: 10.1021/am508854u
ACS Appl. Mater. Interfaces 2015, 7, 1685−1692

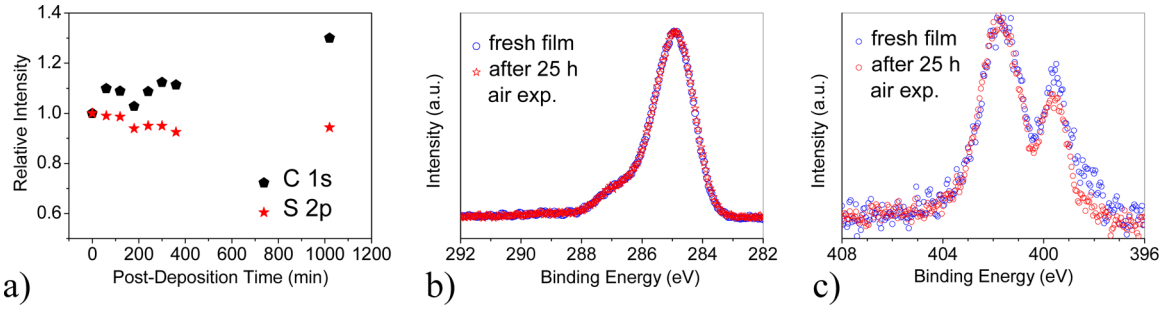

Figure 5. (a) Temporal evolution at room temperature of the Si 2p and C 1s XPS signals for a 1.3 nm nominally thin film after deposition. Comparison of (b) C 1s and (c) N 1s core level spectra of a freshly evaporated film and after 25 h of air exposure.

to transitions to σ^* orbitals (C—C, C═C, and C—N) and shake up contributions ($\pi \rightarrow \pi^*$).[63,64] The shoulder at 286.6 eV may be due to the carbon atoms of the pyrazole ring.[56]

The C−K edge NEXAFS dichroism is useful to calculate the average orientation of the molecular plane of the pyrene substituent with respect to the substrate.[65] The calculation, performed on the resonances at 286.2 eV, yields a value of ∼83°. This orientation of the pyrene substituent is in agreement with the PPN crystal structure,[45] if we assume that the PPN unit cell in the thicker films is arranged with the *b*-axis (i.e., the long axis) almost perpendicular to the substrate surface (Figure 4b). This orientation is very often adopted by molecules in organic thin films deposited on metal oxides.[10,61,66,67]

Figure 4b shows the N−K edge NEXAFS spectrum. It carries information about the radical nature of the molecule because the unpaired electron is delocalized over the two equivalent NO groups. We observe several sharp resonances in the photon energy range between 399 and 404 eV that may be assigned to N 1s→π^* transition contributions according to previous works on NO,[68,69] amino acids,[70] and phthalocyanines.[71−73] The energy range above 405 eV is dominated by a relatively broad peak having σ^* nature due to various contributions including σ^*(N−C).[70] All features in the 398−410 eV energy range have analogy with peak energy and behavior of the features in the N−K edge NEXAFS spectra of small organic molecules. However, we observe an additional signal in the pre-edge region at around 397 eV that, although very weak, may be related to transitions of N−K electrons to the singly occupied molecular orbital (SOMO). The presence of this characteristic feature is not surprising in open shell systems and its intensity might change with the structural properties of the films.[44]

At this point, we intend to discuss two important aspects related to the possible use of PPN in applications, namely, vacuum and air stability of PPN thin films. Two different experiments were set up to explore both aspects using XPS: The first experiment consisted in monitoring PPN films versus time after deposition, taking care of minimizing the beam exposure and switching off the source between the measurements. The second experiment was done by investigating the PPN films before and after air exposure in darkness. Figure 5a shows the time dependence of the Si 2p and C 1s signals. The two signals are substantially stable with a slightly increase of the C 1s signal over 1000 min monitoring, possibly due to the adsorption of carbon from the environment (base pressure of 1×10^{-9} mbar). In Figure 5b, we report the results of the second experiment. Here, after 25 h of air exposure, the films do not show any difference in the C 1s core level spectra. What is most important is that there is no evidence for degradation in the N 1s core level spectra of the nitronyl nitroxide radical exposed to air, because the spectral curves before and after air exposure show no additional signals in the binding energy range around above 402 eV and below 400 eV that would indicate, respectively, either a stronger oxidation of the NO groups or a further release of oxygen atoms. This finding is also quantitatively supported by a best fit procedure (see the Supporting Information).

In our previous studies on NitPyn (in this radical the pyrazole bridging unit between the radical moiety and the fluorophore core is absent, see Scheme 1), we suggested that the use of larger polyaromatic substituents on radicals could be a route to improve the poor vacuum stability of NitPyn films, intrinsically related to the thermodynamics and kinetics of its thin film processes,[39] because it is essential to decrease NitPyn vapor pressure, favoring the growth of organized assemblies. The experimental results that we obtain in the present work clearly support our previous assumptions, and they pave the way to use PPN in future applications such as sensors.[45]

CONCLUSIONS

In conclusion, our work describing the complete electronic structure of thin films of the fluorophore−nitroxide radical PPN demonstrates that this molecule maintains its radical properties in the thin films. Consequently, its sensing capabilities related to the intact nitronyl nitroxide radical are also preserved in the thin film solid state that, in addition, shows a high structural degree of the molecular arrangement. These characteristics are coupled to strong vacuum and air stability, which make PPN an extremely promising candidate for application in electronics. Another remarkable aspect is the possibility to use OMBD to grow PPN thin films: this method allows controlling the growth processes[74] and, consequently, the film characteristics, such as molecular orientation. It is well-known that in organic thin films, the molecular arrangement defines the electronic properties of the systems,[2,75] thus, the use of OMBD that provides fine control and tunability of the molecular arrangement under different preparation conditions,[3,4,10,76−78] can be explored also as a possible tool to influence the magnetic character of the obtained films, by modulating the intermolecular interactions.

Last but not least, our work identifies a strong correlation between the results obtained by the complementary use of XPS and EPR investigations. We prove that this correlation is not only qualitative but, what is more important, also quantitative. This aspect is very useful in order to link the (in situ-measured) electronic structure with classical ex situ paramagnetic investigations.

DOI: 10.1021/am508854u
ACS Appl. Mater. Interfaces 2015, 7, 1685−1692

■ ASSOCIATED CONTENT

Supporting Information

C 1s and N 1s core level spectra of powder PPN embedded in indium foil together with the best fit procedure and the tables of the fitting parameters. Fit results for energy position and relative intensities of the photoemission lines in the C 1s and N 1s spectra for a 3.3 nm nominally thick film. Peak-fit analysis for a freshly evaporated 1.3 nm nominally thin film. C 1s and N 1s peak-fit analysis of the spectra for the 25h air-exposed 1.3 nm nominally thin film. This material is available free of charge via the Internet at http://pubs.acs.org.

■ AUTHOR INFORMATION

Corresponding Author

*M. B. Casu. E-mail: benedetta.casu@uni-tuebingen.de.

Present Address

[§]Institute of Biochemistry, Ernst-Moritz-Arndt University Greifswald, Felix-Hausdorff-Straße 4, 17487 Greifswald, Germany.

Notes

The authors declare no competing financial interest.

■ ACKNOWLEDGMENTS

The authors thank HZB for providing beamtime at BESSY II; W. Neu, E. Nadler, M. Oehzelt, R. Ovsyannikov, and S. Pohl for technical support. Prof. Chassé is gratefully acknowledged for the access to the photoelectron spectroscopy lab of the Condensed Matter Division at the Institute of Physical and Theoretical Chemistry, University of Tübingen. Financial support from Helmholtz-Zentrum Berlin and DFG under the contracts CA852/5-1 and CA852/5-2 is gratefully acknowledged. P.R., Y.B., and M.B. are grateful for support from the SFB TR49.

■ REFERENCES

(1) Tang, C. W.; VanSlyke, S. A. Organic Electroluminescent Diodes. *Appl. Phys. Lett.* **1987**, *51*, 913−915.

(2) Duhm, S.; Heimel, G.; Salzmann, I.; Glowatzki, H.; Johnson, R. L.; Vollmer, A.; Rabe, J. P.; Koch, N. Orientation-Dependent Ionization Energies and Interface Dipoles in Ordered Molecular Assemblies. *Nat. Mater.* **2008**, *7*, 326−332.

(3) Witte, G.; Woll, C. Growth of Aromatic Molecules on Solid Substrates for Applications in Organic Electronics. *J. Mater. Res.* **2004**, *19*, 1889−1916.

(4) Schreiber, F. Organic Molecular Beam Deposition: Growth Studies beyond the First Monolayer. *Phys. Status Solidi A* **2004**, *201*, 1037−1054.

(5) Kronik, L.; Koch, N. Electronic Properties of Organic-based Interfaces. *MRS Bull.* **2010**, *35*, 417−419.

(6) Koch, N. Electronic Structure of Interfaces with Conjugated Organic Materials. *Phys. Status Solidi RRL* **2012**, *6*, 277−293.

(7) Ishii, H.; Sugiyama, K.; Ito, E.; Seki, K. Energy Level Alignment and Interfacial Electronic Structures at Organic/Metal and Organic/Organic Interfaces. *Adv. Mater.* **1999**, *11*, 605−625.

(8) Zahn, D. R. T.; Gavrila, G. N.; Salvan, G. Electronic and Vibrational Spectroscopies Applied to Organic/Inorganic Interfaces. *Chem. Rev. (Washington, DC, U. S.)* **2007**, *107*, 1161−1232.

(9) Casu, M. B.; Schuster, B.-E.; Biswas, I.; Raisch, C.; Marchetto, H.; Schmidt, T.; Chassé, T. Locally Resolved Core-Hole Screening, Molecular Orientation, and Morphology in Thin Films of Diindenoperylene Deposited on Au(111) Single Crystals. *Adv. Mater.* **2010**, *22*, 3740−3744.

(10) Casu, M. B.; Scholl, A.; Bauchspiess, K. R.; Hubner, D.; Schmidt, T.; Heske, C.; Umbach, E. Nucleation in Organic Thin Film Growth: Perylene on $Al_2O_3/Ni_3Al(111)$. *J. Phys. Chem. C* **2009**, *113*, 10990−10996.

(11) Casu, M. B. Nanoscale Order and Structure in Organic Materials: Diindenoperylene on Gold as a Model System. *Cryst. Growth Des.* **2011**, *11*, 3629−3635.

(12) Ueno, N.; Kera, S. Electron Spectroscopy of Functional Organic Thin Films: Deep Insights into Valence Electronic Structure in Relation to Charge Transport Property. *Prog. Surf. Sci.* **2008**, *83*, 490−557.

(13) Heimel, G.; Duhm, S.; Salzmann, I.; Gerlach, A.; Strozecka, A.; Niederhausen, J.; Burker, C.; Hosokai, T.; Fernandez-Torrente, I.; Schulze, G.; Winkler, S.; Wilke, A.; Schlesinger, R.; Frisch, J.; Broker, B.; Vollmer, A.; Detlefs, B.; Pflaum, J.; Kera, S.; Franke, K. J.; Ueno, N.; Pascual, J. I.; Schreiber, F.; Koch, N. Charged and Metallic Molecular Monolayers through Surface-Induced Aromatic Stabilization. *Nat. Chem.* **2013**, *5*, 187−194.

(14) Häming, M.; Schöll, A.; Umbach, E.; Reinert, F. Adsorbate-Substrate Charge Transfer and Electron-Hole Correlation at Adsorbate/Metal Interfaces. *Phys. Rev. B* **2012**, *85*, 235132.

(15) Tseng, T.-C.; Urban, C.; Wang, Y.; Otero, R.; Tait, S. L.; Alcamí, M.; Écija, D.; Trelka, M.; Gallego, J. M.; Lin, N.; Konuma, M.; Starke, U.; Nefedov, A.; Langner, A.; Wöll, C.; Herranz, M. Á.; Martín, F.; Martín, N.; Kern, K.; Miranda, R. Charge-Transfer-Induced Structural Rearrangements at Both Sides of Organic/Metal Interfaces. *Nat. Chem.* **2010**, *2*, 374−379.

(16) Braun, S.; Salaneck, W. R.; Fahlman, M. Energy-Level Alignment at Organic/Metal and Organic/Organic Interfaces. *Adv. Mater.* **2009**, *21*, 1450−1472.

(17) Anthony, J. E. Functionalized Acenes and Heteroacenes for Organic Electronics. *Chem. Rev. (Washington, DC, U. S.)* **2006**, *106*, 5028−5048.

(18) Klauk, H. Organic Thin-Film Transistors. *Chem. Soc. Rev.* **2010**, *39*, 2643−2666.

(19) Tautz, F. S. Structure and Bonding of Large Aromatic Molecules on Noble Metal Surfaces: The Example of PTCDA. *Prog. Surf. Sci.* **2007**, *82*, 479−520.

(20) Knupfer, M.; Peisert, H. Electronic Properties of Interfaces between Model Organic Semiconductors and Metals. *Phys. Status Solidi A* **2004**, *201*, 1055−1074.

(21) Shirota, Y. Organic Materials for Electronic and Optoelectronic Devices. *J. Mater. Chem.* **2000**, *10*, 1−25.

(22) Guo, X.; Baumgarten, M.; Mullen, K. Designing π-Conjugated Polymers for Organic Electronics. *Prog. Polym. Sci.* **2013**, *38*, 1832−1908.

(23) Gallani, J. L.; Le Moigne, J.; Oswald, L.; Bernard, M.; Turek, P. Induced Ferromagnetic Interactions in Langmuir−Blodgett Films of an Organic Radical. *Langmuir* **2001**, *17*, 1104−1109.

(24) Matsushita, M. M.; Ozaki, N.; Sugawara, T.; Nakamura, F.; Hara, M. Formation of Self-Assembled Monolayer of Phenylthiol Carrying Nitronyl Nitroxide on Gold Surface. *Chem. Lett.* **2002**, *31*, 596−597.

(25) Mannini, M.; Sorace, L.; Gorini, L.; Piras, F. M.; Caneschi, A.; Magnani, A.; Menichetti, S.; Gatteschi, D. Self-Assembled Organic Radicals on Au(111) Surfaces: A Combined TOF-SIMS, STM, and ESR Study. *Langmuir* **2007**, *23*, 2389−2397.

(26) Mannini, M.; Rovai, D.; Sorace, L.; Perl, A.; Ravoo, B. J.; Reinhoudt, D. N.; Caneschi, A. Patterned Monolayers of Nitronyl Nitroxide Radicals. *Inorg. Chim. Acta* **2008**, *361*, 3525−3528.

(27) Gatteschi, D.; Cornia, A.; Mannini, M.; Sessoli, R. Organizing and Addressing Magnetic Molecules. *Inorg. Chem.* **2009**, *48*, 3408−3419.

(28) Mas-Torrent, M.; Crivillers, N.; Rovira, C.; Veciana, J. Attaching Persistent Organic Free Radicals to Surfaces: How and Why. *Chem. Rev. (Washington, DC, U. S.)* **2011**, *112*, 2506−2527.

(29) Fraxedas, J.; Caro, J.; Santiso, J.; Figueras, A.; Gorostiza, P.; Sanz, F. Polymorphic Transformations Observed on Molecular Organic Thin Films: p-Nitrophenyl Nitronyl Nitroxide Radical. *Europhys. Lett.* **1999**, *48*, 461.

DOI: 10.1021/am508854u
ACS Appl. Mater. Interfaces 2015, 7, 1685−1692

(30) Molas, S.; Coulon, C.; Fraxedas, J. Magnetic Properties of Thin α-p-Nitrophenyl Nitronyl Nitroxide Films. *CrystEngComm* **2003**, *5*, 310−312.
(31) Blinco, J. P.; Chalmers, B. A.; Chou, A.; Fairfull-Smith, K. E.; Bottle, S. E. Spin-Coated Carbon. *Chem. Sci.* **2013**, *4*, 3411−3415.
(32) Osiecki, J. H.; Ullman, E. F. Studies of Free Radicals. I. α-Nitronyl Nitroxides, A New Class of Stable Radicals. *J. Am. Chem. Soc.* **1968**, *90*, 1078−1079.
(33) Tamura, M.; Nakazawa, Y.; Shiomi, D.; Nozawa, K.; Hosokoshi, Y.; Ishikawa, M.; Takahashi, M.; Kinoshita, M. Bulk Ferromagnetism in the β-Phase Crystal of the p-Nitrophenyl Nitronyl Nitroxide Radical. *Chem. Phys. Lett.* **1991**, *186*, 401−404.
(34) Caneschi, A.; Gatteschi, D.; Sessoli, R.; Rey, P. Toward Molecular Magnets: The Metal-Radical Approach. *Acc. Chem. Res.* **1989**, *22*, 392−398.
(35) Veciana, J.; Iwamura, H. Organic Magnets. *MRS Bull.* **2000**, *25*, 41−51.
(36) Ratera, I.; Veciana, J. Playing with Organic Radicals as Building Blocks for Functional Molecular Materials. *Chem. Soc. Rev.* **2012**, *41*, 303−349.
(37) Ravat, P.; Marszalek, T.; Pisula, W.; Müllen, K.; Baumgarten, M. Positive Magneto-LC Effect in Conjugated Spin-Bearing Hexabenzocoronene. *J. Am. Chem. Soc.* **2014**, *136*, 12860−12863.
(38) Lee, J.; Lee, E.; Kim, S.; Bang, G. S.; Shultz, D. A.; Schmidt, R. D.; Forbes, M. D. E.; Lee, H. Nitronyl Nitroxide Radicals as Organic Memory Elements with Both n- and p-Type Properties. *Angew. Chem., Int. Ed.* **2011**, *50*, 4414−4418.
(39) Savu, S.-A.; Biswas, I.; Sorace, L.; Mannini, M.; Rovai, D.; Caneschi, A.; Chassé, T.; Casu, M. B. Nanoscale Assembly of Paramagnetic Organic Radicals on Au(111) Single Crystals. *Chem.—Eur. J.* **2013**, *19*, 3445−3450.
(40) Caneschi, A.; Casu, M. B. Substrate-Induced Effects in Thin Films of a Potential Magnet Composed of Metal-Free Organic Radicals Deposited on Si(111). *Chem. Commun. (Cambridge, U. K.)* **2014**, *50*, 13510−13513.
(41) Kakavandi, R.; Savu, S.-A.; Sorace, L.; Rovai, D.; Mannini, M.; Casu, M. B. Core-Hole Screening, Electronic Structure, and Paramagnetic Character in Thin Films of Organic Radicals Deposited on Sio2/Si(111). *J. Phys. Chem. C* **2014**, *118*, 8044−8049.
(42) Abb, S.; Savu, S.-A.; Caneschi, A.; Chassé, T.; Casu, M. B. Paramagnetic Nitronyl Nitroxide Radicals on Al_2O_3(11−20) Single Crystals: Nanoscale Assembly, Morphology, Electronic Structure, and Paramagnetic Character toward Future Applications. *ACS Appl. Mater. Interfaces* **2013**, *5*, 13006−13011.
(43) Kakavandi, R.; Savu, S.-A.; Caneschi, A.; Chasse, T.; Casu, M. B. At the Interface between Organic Radicals and TiO_2(110) Single Crystals: Electronic Structure and Paramagnetic Character. *Chem. Commun. (Cambridge, U. K.)* **2013**, *49*, 10103−10105.
(44) Kakavandi, R.; Savu, S.-A.; Caneschi, A.; Casu, M. B. Paramagnetic Character in Thin Films of Metal-Free Organic Magnets Deposited on TiO_2(110) Single Crystals. *J. Phys. Chem. C* **2013**, *117*, 26675−26679.
(45) Borozdina, Y. B.; Kamm, V.; Laquai, F.; Baumgarten, M. Tuning the Sensitivity of Fluorophore-Nitroxide Radicals. *J. Mater. Chem.* **2012**, *22*, 13260−13267.
(46) Blinco, J. P.; Fairfull-Smith, K. E.; Morrow, B. J.; Bottle, S. E. Profluorescent Nitroxides as Sensitive Probes of Oxidative Change and Free Radical Reactions. *Aust. J. Chem.* **2011**, *64*, 373−389.
(47) Likhtenshtein, G. Novel Fluorescent Methods for Biotechnological and Biomedical Sensoring: Assessing Antioxidants, Reactive Radicals, No Dynamics, Immunoassay, and Biomembranes Fluidity. *Appl. Biochem. Biotechnol.* **2009**, *152*, 135−155.
(48) Wang, H.; Zhang, D.; Guo, X.; Zhu, L.; Shuai, Z.; Zhu, D. Tuning the Fluorescence of 1-Imino Nitroxide Pyrene with Two Chemical Inputs: Mimicking the Performance of an "AND" Gate. *Chem. Commun. (Cambridge, U. K.)* **2004**, 670−671.
(49) Hughes, B. K.; Braunecker, W. A.; Ferguson, A. J.; Kemper, T. W.; Larsen, R. E.; Gennett, T. Quenching of the Perylene Fluorophore by Stable Nitroxide Radical-Containing Macromolecules. *J. Phys. Chem. B* **2014**, *118*, 12541−12548.
(50) Ohring, M. *Materials Science of Thin Films*; Academic Press: San Diego, 2002.
(51) Verlaak, S.; Steudel, S.; Heremans, P.; Janssen, D.; Deleuze, M. S. Nucleation of Organic Semiconductors on Inert Substrates. *Phys. Rev. B* **2003**, *68*, 195409.
(52) Hesse, R.; Chassé, T.; Streubel, P.; Szargan, R. Error Estimation in Peak-Shape Analysis of XPS Core-Level Spectra Using Unifit 2003: How Significant Are the Results of Peak Fits? *Surf. Interface Anal.* **2004**, *36*, 1373−1383.
(53) Casu, M. B.; Chassé, T. *Photoelectron Spectroscopy Applications to Materials Science*, Second ed.; Wiley-VCH: Weinheim, Germany, 2014.
(54) Baumgarten, M. *EPR of Free Radicals in Solids*; Kluwer Academics Publishers: Dordrecht, The Netherlands, 2003.
(55) Weil, J. A.; Bolton, J. R.; Wertz, J. E. *Electron Paramagnetic Resonance, Elementary Theory and Practical Applications*; Wiley: New York, 1994.
(56) Shen, C.; Haryono, M.; Grohmann, A.; Buck, M.; Weidner, T.; Ballav, N.; Zharnikov, M. Self-Assembled Monolayers of a Bis(pyrazol-1-yl)pyridine-Substituted Thiol on Au(111). *Langmuir* **2008**, *24*, 12883−12891.
(57) Dementjev, A. P.; de Graaf, A.; van de Sanden, M. C. M.; Maslakov, K. I.; Naumkin, A. V.; Serov, A. A. X-ray Photoelectron Spectroscopy Reference Data for Identification of the C_3N_4 Phase in Carbon−Nitrogen Films. *Diamond Relat. Mater.* **2000**, *9*, 1904−1907.
(58) Jansen, R. J. J.; van Bekkum, H. XPS of Nitrogen-Containing Functional Groups on Activated Carbon. *Carbon* **1995**, *33*, 1021−1027.
(59) Gammon, W. J.; Kraft, O.; Reilly, A. C.; Holloway, B. C. Experimental Comparison of N(1s) X-ray Photoelectron Spectroscopy Binding Energies of Hard and Elastic Amorphous Carbon Nitride Films with Reference Organic Compounds. *Carbon* **2003**, *41*, 1917−1923.
(60) Ravat, P.; Ito, Y.; Gorelik, E.; Enkelmann, V.; Baumgarten, M. Tetramethoxypyrene-based Biradical Donors with Tunable Physical and Magnetic Properties. *Org. Lett.* **2013**, *15*, 4280−4283.
(61) Schuster, B.-E.; Casu, M. B.; Biswas, I.; Hinderhofer, A.; Gerlach, A.; Schreiber, F.; Chassé, T. Role of the Substrate in Electronic Structure, Molecular Orientation, and Morphology of Organic Thin Films: Diindenoperylene on Rutile TiO_2(110). *Phys. Chem. Chem. Phys.* **2009**, *11*, 9000−9004.
(62) Winkler, S.; Frisch, J.; Schlesinger, R.; Oehzelt, M.; Rieger, R.; Räder, J.; Rabe, J. P.; Müllen, K.; Koch, N. The Impact of Local Work Function Variations on Fermi Level Pinning of Organic Semiconductors. *J. Phys. Chem. C* **2013**, *117*, 22285−22289.
(63) Sandi, G.; Song, K.; Carrado, K. A.; Winans, R. E. A NEXAFS Determination of the Electronic Structure of Carbons for Lithium-Ion Cells. *Carbon* **1998**, *36*, 1755−1758.
(64) Lucas, L. A.; DeLongchamp, D. M.; Richter, L. J.; Kline, R. J.; Fischer, D. A.; Kaafarani, B. R.; Jabbour, G. E. Thin Film Microstructure of a Solution Processable Pyrene-based Organic Semiconductor. *Chem. Mater.* **2008**, *20*, 5743−5749.
(65) Stöhr, J.; Outka, D. A. Determination of Molecular Orientations on Surfaces from the Angular Dependence of near-Edge X-ray-Absorption Fine-Structure Spectra. *Phys. Rev. B* **1987**, *36*, 7891−7905.
(66) Liscio, F.; Albonetti, C.; Broch, K.; Shehu, A.; Quiroga, S. D.; Ferlauto, L.; Frank, C.; Kowarik, S.; Nervo, R.; Gerlach, A.; Milita, S.; Schreiber, F.; Biscarini, F. Molecular Reorganization in Organic Field-Effect Transistors and Its Effect on Two-Dimensional Charge Transport Pathways. *ACS Nano* **2013**, *7*, 1257−1264.
(67) Kowarik, S.; Gerlach, A.; Sellner, S.; Schreiber, F.; Cavalcanti, L.; Konovalov, O. Real-Time Observation of Structural and Orientational Transitions During Growth of Organic Thin Films. *Phys. Rev. Lett.* **2006**, *96*, 125504.
(68) Saito, T.; Imamura, M.; Matsubayashi, N.; Furuya, K.; Kikuchi, T.; Shimada, H. Geometric and Electronic Structures of NO Adsorbed on Ni, Rh and Pt Studied by Using near Edge X-ray Absorption Fine

DOI: 10.1021/am508854u
ACS Appl. Mater. Interfaces 2015, 7, 1685−1692

Structure (NEXAFS) and Resonant Photoemission Spectroscopy. *J. Electron Spectrosc. Relat. Phenom.* **2001**, *119*, 95−105.
(69) Morgante, A.; Cvetko, D.; Santoni, A.; Prince, K. C.; Dhanak, V. R.; Comelli, G.; Kiskinova, M. A Synchrotron Radiation Study of NO and Oxygen on Rh(110). *Surf. Sci.* **1993**, *285*, 227−236.
(70) Zubavichus, Y.; Shaporenko, A.; Grunze, M.; Zharnikov, M. Innershell Absorption Spectroscopy of Amino Acids at All Relevant Absorption Edges. *J. Phys. Chem. A* **2005**, *109*, 6998−7000.
(71) Biswas, I.; Peisert, H.; Nagel, M.; Casu, M. B.; Schuppler, S.; Nagel, P.; Pellegrin, E.; Chassé, T. Buried Interfacial Layer of Highly Oriented Molecules in Copper Phthalocyanine Thin Films on Polycrystalline Gold. *J. Chem. Phys.* **2007**, *126*, 174704.
(72) Kera, S.; Casu, M. B.; Schoell, A.; Schmidt, T.; Batchelor, D.; Ruehl, E.; Umbach, E. High-Resolution Inner-Shell Excitation Spectroscopy of H-2-Phthalocyanine. *J. Chem. Phys.* **2006**, *125*, 014705.
(73) Kera, S.; Casu, M. B.; Bauchspiess, K. R.; Batchelor, D.; Schmidt, T.; Umbach, E. Growth Mode and Molecular Orientation of Phthalocyanine Molecules on Metal Single Crystal Substrates: A NEXAFS and XPS Study. *Surf. Sci.* **2006**, *600*, 1077−1084.
(74) Forrest, S. R. Ultrathin Organic Films Grown by Organic Molecular Beam Deposition and Related Techniques. *Chem. Rev. (Washington, DC, U. S.)* **1997**, *97*, 1793−1896.
(75) Kolata, K.; Breuer, T.; Witte, G.; Chatterjee, S. Molecular Packing Determines Singlet Exciton Fission in Organic Semiconductors. *ACS Nano* **2014**, *8*, 7377−7383.
(76) Casu, M. B.; Yu, X.; Schmitt, S.; Heske, C.; Umbach, E. Morphology of Perylene Thin Films on SiO_x/Si(100) and SiO_2/Si(100): A Spectroscopic and Microscopic Study of the Influence of the Preparation Parameters. *Chem. Phys. Lett.* **2009**, *479*, 76−80.
(77) Casu, M. B.; Yu, X.; Schmitt, S.; Heske, C.; Umbach, E. Influence of the Preparation Conditions on the Morphology of Perylene Thin Films on Si(111) and Si(100). *J. Chem. Phys.* **2008**, *129*, 244708−244708.
(78) Witte, G.; Wöll, C. Molecular Beam Deposition and Characterization of Thin Organic Films on Metals for Applications in Organic Electronics. *Phys. Status Solidi A* **2008**, *205*, 497−510.

DOI: 10.1021/am508854u
ACS Appl. Mater. Interfaces 2015, 7, 1685−1692